J|A|C|S
COMMUNICATIONS

Published on Web 11/17/2005

Substrate-Induced Raman Frequency Variation for Single-Walled Carbon Nanotubes

Yingying Zhang,[†] Jin Zhang,*[,†] Hyungbin Son,[‡] Jing Kong,*[,‡] and Zhongfan Liu*[,†]

Centre for Nanoscale Science and Technology, Key Laboratory for the Physics and Chemistry of Nanodevices, College of Chemistry and Molecular Engineering, Peking University, Beijing 100871, P. R. China, and Department of Electrical Engineering and Computer Science, Massachusetts Institute of Technology, Cambridge, Massachusetts 02139

Received October 5, 2005; E-mail: jinzhang@pku.edu.cn

During the past few years, resonant Raman spectroscopy has been developed into a powerful tool for characterizing the structure of carbon nanotubes.[1] Particularly, it was demonstrated that by comparing the experimental resonant energy E_{ii} and the radial-breathing mode (RBM) frequency ω_{RBM} with the theoretically calculated Kataura plot, it is possible to determine the chirality (n,m) of an individual single-walled nanotube (SWNT).[2] As these values can be significantly affected by the surrounding environment of a SWNT, to ensure the accuracy of the chirality identification, it is very important to find out how various environmental conditions alter the E_{ii} or ω_{RBM} values. Recent studies have shown that the ω_{RBM} values are relatively insensitive to the type of wrapping agents surrounding the nanotube in a solution.[3] Various calculations have predicted changes in the electronic band structure of nanotubes under strain.[4] Raman frequency shifts due to applied uniaxial strain have also been observed.[5] Another important source of perturbation is the van der Waals interactions with the substrate. However, it is still an open question to what extent these interactions will affect the SWNT's E_{ii} or ω_{RBM}.

In this paper, we report on the frequency shift of the Raman spectra taken at different locations along the same SWNT, showing different results when the SWNT is freely suspended or when interacting with the substrate. The substrates used in this study are silicon wafers with thermal oxide on the surface, which contains trenches (300 nm deep, 1−80 μm wide) fabricated by photolithography and dry etching (Figure 1). Well separated, individual long SWNTs with a controlled orientation were grown by catalytic chemical vapor decomposition (CVD) of ethanol[6] (see Supporting Information for details). An SEM image of the carbon nanotubes thus obtained is shown in Figure 1b. As shown by atomic force microscopy (AFM), nanotubes are suspended over trenches narrower than 3 μm (see Figure 1c and Figure S1).

Raman spectra of the same SWNTs were collected and compared as the laser beam moved along the nanotube. With an excitation energy of 1.96 eV (633 nm), all the SWNTs that came into resonance demonstrated a stronger signal for the suspended part than the part sitting on the SiO_2 surface, which is consistent with what has been reported in the literature.[7] More interesting, for several of the nanotubes, the Raman signals (RBM and G-band) showed an obvious upshift in the frequency of ω_{RBM} and ω_G when the laser beam was moved from the middle of the trench to the SiO_2 surface along the nanotube axis. These shifts could be as large as 12 cm^{-1} and appear to be observed with nanotubes having relatively large diameter, that is, close to 2 nm.

Figure 2 shows representative Raman spectra of a SWNT with a diameter of ~1.8 nm. Numbers 1−7 label the position of the laser spot moving from the middle of the trench to the SiO_2 substrate. Each step is 500 nm, and the Raman spectrum taken at each location is plotted with a different color. Graphs a and b in Figure 2 show the region near the G-band and RBM, respectively. In the inset of Figure 2b, Raman signals are taken with the focusing spot moving from the middle of trench to the right side. Figure 2b and its inset demonstrated similar results, indicating that this kind of Raman frequency variation is intrinsic to the nanotube. For most of the Raman spectra of the SWNTs in this study, there is no observable D-band, demonstrating the high quality of these SWNTs and, in addition, excluding the possibility that this kind of shift is due to the defects in the nanotubes. Along with the frequency shift, the intensity changes monotonically, and it is more than 20 times stronger for the suspended part of the SWNT than that sitting on top of the SiO_2 surface. There are two possible reasons giving rise to the intensity variation: the first is that the resonant energy E_{ii} changed when the nanotube is sitting on top of the SiO_2 as compared to the freely suspended part due to the van der Waals SWNT−SiO_2 interactions,[8] and therefore, the freely suspended part is in stronger resonance than the part having interactions with substrate; the second is that the substrate interaction suppresses the Raman intensity. Currently, we are studying these samples with a tunable

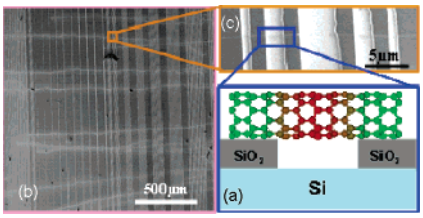

Figure 1. (a) Schematic illustration for a SWNT lying on a patterned SiO_2 substrate. Our samples have various trench widths. All the data presented here are from nanotubes lying over the 3 μm wide trenches. (b) SEM image of the ultralong carbon nanotube sample used for the Raman investigations. (c) High-resolution SEM image of one SWNT lying over the trenches. (In the SEM image, lighter color indicates the trench.)

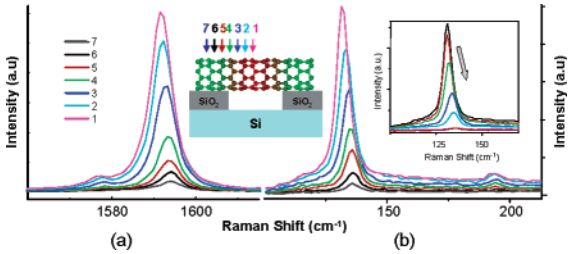

Figure 2. Typical Raman spectra of the same SWNT with the laser spot moving along the tube from the middle of the trench to the left side. (a) G-band (G^+/G^- from 1591.6/1575.7 to 1594.2/1578.3 cm^{-1}). (b) RBM (from 131.4 to 136.9 cm^{-1}). The left inset gives the legend for the laser spot moving in a backward direction, and the right inset shows the RBM spectra when the laser beam moves from the middle of the trench to the right side.

[†] Peking University.
[‡] Massachusetts Institute of Technology.

10.1021/ja056793c CCC: $30.25

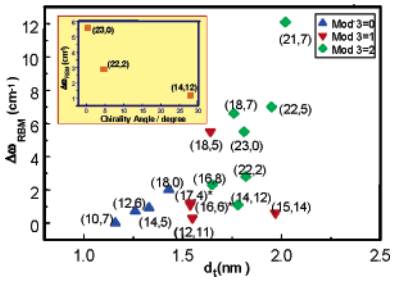

Figure 3. The dependence of $\Delta\omega_{RBM}$ on d_t. Three types of symbols represent three types of SWNTs ($(n - m)\text{mod}3 = 0$, $(n - m)\text{mod}3 = 1$, and $(n - m)\text{mod}3 = 2$). Inset is $\Delta\omega_{RBM}$ versus the chiral angle for three SWNTs with similar diameter. Symbols $*$ indicate that three SWNTs ((17,4) and two (16,6)) are too close to be identified in the figure.

excitation source around 633 nm to identify the main reason for the intensity variation.

Compared with the intensity changes, the frequency shift, especially the RBM shift, appears to be rather surprising. If we take the Raman frequency of the freely suspended part as the intrinsic "reference" point, the upshift of the signals on SiO_2 appear to be a "mode hardening" effect. A number of possibilities can lead to this hardening effect. The first is a heating effect,[9] where the frequency downshift for the suspended part over the trench indicates that this part should experience a severe heating effect compared to the part on the SiO_2. However, from our studies (data not shown), since the absorption cross-section of a SWNT is very small, only nanotubes that are supported on a substrate can be heated by laser beam through the heating of the substrate. In addition, we have tried different laser power levels at the same locations, and the peak frequencies did not change when changing the laser power (See Figure S2 in Supporting Information), thus eliminating the possibility of a heating effect. Another commonly observed cause of Raman frequency variation is the doping effect. Various chemical[10] or electrochemical[11] doping studies have been carried out on SWNTs, and their Raman frequencies have been reported to shift due to the transfer of charge carriers. However, considering the fact that SiO_2 is a rather insulating material, the frequency upshift on SiO_2 compared with the freely suspended part implies significant electron donation from SiO_2 to the nanotubes, which is very unlikely. The last possibility, which we think plays a primary role in our system, is radial deformation induced by nanotube−substrate van der Waals interactions,[8] which destroy the idealized shape of a free tube and distort the SWNT cross-section from a circle to an ellipse. Moreover, considering the high temperature process during nanotube preparation, an enhanced nanotube−substrate interaction may be conceivable. Previous work indicates that the extent of radial deformation through surface van der Waals forces increases dramatically with increasing tube diameter (d_t).[8] We have collected Raman data on 17 individual SWNTs and summarized the data (see Table S1 in Supporting Information). The dependence of $\Delta\omega_{RBM}$ (shift of ω_{RBM}) on d_t (calculated according $d_t = 248/\omega_{RBM}$,[2] using the ω_{RBM} of the part sitting on SiO_2) is plotted in Figure 3. A clear trend can be seen that all large $\Delta\omega_{RBM}$ are related to tubes with relatively large d_t, and no large shift of ω_{RBM} occurs for small d_t nanotubes. These results are in good agreement with theoretical results on radial deformation[8] and further confirm our proposed scenario.

It is worth noting that not all the large diameter tubes gave a large $\Delta\omega_{RBM}$, suggesting this effect is chirality dependent. We made a tentative (n,m) assignment for all 17 SWNTs (see Supporting Information for details) and found that for tubes with similar d_t, $\Delta\omega_{RBM}$ tended to increase with decreasing θ, as shown in the inset of Figure 3. These facts are consistent with calculated results, which suggested that radial deformation is chirality dependent.[12] In addition, in Figure 3, most of the large shifts are related to $(n - m)\text{mod}3 = 2$ semiconducting nanotubes (marked with green diamond), which indicates this effect is not universal but is rather specific to a particular type of nanotubes.

In our observed frequency shifts, there does not appear to be a correlation between the magnitude of $\Delta\omega_{RBM}$ and $\Delta\omega_G$. Previous work has suggested that under axial strain, the relative change of ω_{RBM} is related to the corresponding shift of the ω_{G+} as $\Delta\omega_{RBM}/\omega_{RBM} = 0.15\Delta\omega_{G+}/\omega_{G+}$.[13] This result is quite different from our experiment. The G-band, related to the carbon−carbon stretching motion in the tangential direction of the nanotube, is sensitive to axial strain, while the RBM depends primarily on strain in the radial direction since it corresponds to the in-phase vibration of carbon atoms in a direction perpendicular to the tube axis. So a relatively larger $\Delta\omega_{RBM}$ and a relatively smaller $\Delta\omega_G$ in our experiment indicate that the origin of strain in our system is mainly driven by radial deformation. Additionally, in a recent work,[5] examining the axial strain of SWNTs by AFM manipulation, the ω_{RBM} remains unchanged even when the shift of ω_G is as large as 40 cm^{-1}. The striking contrast between their results and ours further confirms that it is radial strain that plays a predominant role for the shift of the ω_{RBM} in our experiment.

In summary, we have observed a dramatic Raman frequency variation for the same SWNT due to its radial deformation when lying on the substrate. The effect is more obvious with larger diameter nanotubes and appears to be chirality dependent. Our results shed new light into environmental effects on the properties of carbon nanotubes, and further investigations are underway to reveal the E_{ii} variations due to these interactions with substrates.

Acknowledgment. This work was supported by NSFC (90206023) and MOST(2001CB6105). We are grateful to Prof. M. S. Dresselhaus (MIT), Prof. G. Dresselhaus (MIT), and Prof. T. Zhu (PKU) for helpful discussions. H.S. and J.K. gratefully acknowledge support from Intel High Education Program.

Supporting Information Available: A description of the sample preparation; an AFM image of the suspended nanotubes (Figure S1); laser power dependence of the RBM frequency shift (Figure S2); summary of the frequency shifts and chirality assignments (Table S1); and complete author list of references. This material is available free of charge via the Internet at http://pubs.acs.org.

References

(1) Dresselhaus, M. S.; Dresselhaus, G.; Saito, R.; Jorio, A. *Phys. Rep.* **2005**, *409*, 47−99.
(2) Jorio, A.; Saito, R.; Hafner, J. H.; Lieber, C. M.; McClure, T.; Dresselhaus, G.; Dresselhaus, M. S. *Phys. Rev. Lett.* **2001**, *86*, 1118−1121.
(3) Chou, S. G. et al. *Chem. Phys. Lett.* **2004**, *397*, 296−301.
(4) Ogata, S.; Shibutani, Y. *Phys. Rev. B* **2003**, *68*, 165409.
(5) Cronin, S. B.; Swan, A. K.; Unlu, M. S.; Goldberg, B. B.; Dresselhaus, M. S.; Tinkham, M. *Phys. Rev. Lett.* **2004**, *93*, 167401.
(6) Zheng, L. X.; O'Connell, M. J.; Doorn, S. K.; Liao, X. Z.; Zhao, Y. H.; Akhadov, E. A.; Hoffbauer, M. A.; Roop, B. J.; Jia, Q. X.; Dye, R. C.; Peterson, D. E.; Huang, S. M.; Liu, J.; Zhu, Y. T. *Nat. Mater.* **2004**, *3*, 673−676.
(7) Son, H. B.; Hori, Y.; Chou, S. G.; Nezich, D.; Samsonidze, G. G.; Dresselhaus, G.; Dresselhaus, M. S.; Barros, E. B. *Appl. Phys. Lett.* **2004**, *85*, 4744−4746.
(8) Hertel, T.; Walkup, R. E.; Avouris, P. *Phys. Rev. B* **1998**, *58*, 13870−13873.
(9) Raravikar, N. R.; Keblinski, P.; Rao, A. M.; Dresselhaus, M. S.; Schadler, L. S. *Phys. Rev. B* **2002**, *66*, 235424.
(10) Rao, A. M.; Eklund, P. C.; Bandow, S.; Thess, A.; Smalley, R. E. *Nature* **1997**, *388*, 357−259.
(11) Kavan, L.; Rapta, P.; Dunsch, L.; Bronikowski, M. J.; Willis, P.; Smalley, R. E. *J. Phys. Chem. B* **2001**, *105*, 10764−10771.
(12) (a) Fa, W.; Hu, F.; Dong, J. *Phys. Lett. A* **2004**, *331*, 99−104. (b) Lammert, P. E.; Zhang, P.; Crespi, V. H. *Phys. Rev. Lett.* **2000**, *84*, 2453−2456.
(13) Hadjiev, V. G.; Mitchell, C. A.; Arepalli, S.; Bahr, J. L.; Tour, J. M.; Krishnamoorti, R. *J. Chem. Phys.* **2005**, *122*, 124708.

JA056793C